



# Effect of Organic Alkalinity on Seawater Buffer Capacity: A Numerical Exploration

Xinping Hu<sup>1</sup>

Received: 18 September 2019 / Accepted: 9 April 2020  
© Springer Nature B.V. 2020

## Abstract

Organic alkalinity is a poorly understood component of total titration alkalinity in aquatic environments. Using a numerical method, the effects of organic acid (HOA) and its conjugate base ( $\text{OA}^-$ ) on seawater carbonate chemistry and buffer behaviors, as well as those in a hypothetical estuarine mixing zone, are explored under both closed- and open-system conditions. The simulation results show that HOA addition leads to  $p\text{CO}_2$  increase and pH decrease in a closed system when total dissolved inorganic carbon (DIC) remains the same. If opened to the atmosphere ( $p\text{CO}_2 = 400 \text{ \mu atm}$ ),  $\text{CO}_2$  degassing and re-equilibration would cause depressed pH compared to the unperturbed seawater, but the seawater buffer to pH change  $\left( \beta_{\text{DIC}} = \left( \frac{\partial \ln([H^+])}{\partial \text{DIC}} \right)^{-1} \right)$  indicates that weaker organic acid (i.e., higher  $pK_a$ ) results in higher buffer capacity (greater  $\beta_{\text{DIC}}$ ) than the unperturbed seawater. In comparison,  $\text{OA}^-$  (with accompanying cations) in the form of net alkalinity addition leads to  $p\text{CO}_2$  decrease in a closed system. After re-equilibrating with the atmosphere, the resulting perturbed seawater has higher pH and  $\beta_{\text{DIC}}$  than the unperturbed seawater. If river water has organic alkalinity, pH in the estuarine mixing zone is always lower than those caused by a mixing between organic alkalinity-free river (at constant total alkalinity) and ocean waters, regardless of the  $pK_a$  values. On the other hand, organic alkalinity with higher  $pK_a$  provides slightly greater  $\beta_{\text{DIC}}$  in the mixing zone, and that with lower  $pK_a$  either results in large  $\text{CO}_2$  oversaturation (closed system) or reduced  $\beta_{\text{DIC}}$  (in mid to high salinity in the closed system or the entire mixing zone in the open system). Finally, despite the various effects on seawater buffer through either HOA or  $\text{OA}^-$  addition, destruction of organic molecules including organic alkalinity via biogeochemical reactions should result in a net  $\text{CO}_2$  loss from seawater. Nevertheless, the significance of this organic alkalinity, especially that comes from organic acids that are not accounted for under the currently recognized “zero proton level” (Dickson in Deep Sea Res 28:609–623, 1981), remains unknown thus a potentially interesting and relevant research topic in studying oceanic alkalinity cycle.

---

**Electronic supplementary material** The online version of this article (<https://doi.org/10.1007/s10498-020-09375-x>) contains supplementary material, which is available to authorized users.

✉ Xinping Hu  
xinpinglei@tamu.edu

<sup>1</sup> Department of Physical and Environmental Sciences, Texas A&M University-Corpus Christi, Corpus Christi, TX 78412, USA

**Keywords** Organic alkalinity · Buffer · Carbonate chemistry · Ocean acidification

## 1 Introduction

Numerous studies (e.g., Hagens et al. 2014; Hofmann et al. 2010) have investigated the responses of the seawater acid–base buffer system to environmental perturbations such as the ocean acidification following the classic work by Revelle and Suess (1957). As pH is the “master variable” in the seawater media (Jourabchi et al. 2005) and can be measured directly, determining how proton concentration changes as a result of ocean acidification has been one of the focal points in numerous studies (Egleston et al. 2010; Frankignoulle 1994; Hagens and Middelburg 2016; Hofmann et al. 2010). Therefore, elucidating the buffer mechanisms that control the magnitude of proton concentration changes due to biogeochemical reactions is important for understanding the seawater acid–base properties under the changing ocean conditions.

Among the many acid–base pairs that contribute to seawater buffer under normal oxic conditions, carbonate, borate, and nutrients (ammonia, phosphate, and silicate) have been studied extensively and are well documented (Hagens and Middelburg 2016). It is known that the carbonate species ( $\text{HCO}_3^-$  and  $\text{CO}_3^{2-}$ ) contribute the most to the buffer capacity in seawater and borate ( $\text{B}(\text{OH})_4^-$  and  $\text{H}_3\text{BO}_3$ ) follows (Stumm and Morgan 1995). With the exception of anoxic environments (sediment porewater or water column in anoxic basins), nutrients and sulfide do not provide significant buffer (Ben-Yakov 1973; Boudreau and Canfield 1993). In addition to the inorganic acid–base pairs, organic acids, their dissociation products (the conjugate bases of organic acids are considered as organic alkalinity), plankton, and bacteria cells have all been proposed to provide buffer in seawater (Kim et al. 2006). Hence, while the global oceans are under the threat of ocean acidification, organic alkalinity is also proposed to provide additional buffer, at least in the coastal ocean where organic levels are high relative to the open ocean (Sippo et al. 2016).

Organic alkalinity is not a new concept and has long been recognized as a possible component of total titration alkalinity in seawater (e.g., Dickson 1992). As rivers are known to carry non-trivial amounts of organic acids (e.g., Perdue et al. 1980; Ritchie and Perdue 2003), their conjugate bases contribute to alkalinity in both river and coastal waters (Cai et al. 1998; Hunt et al. 2011). In recent years, organic alkalinity has been receiving increasing attention in not only the water column (Hammer et al. 2017; Hernández-Ayon et al. 2007; Kim and Lee 2009; Ko et al. 2016; Kuliński et al. 2014; Muller and Bleie 2008; Wang et al. 2013; Yang et al. 2015), but also sediment pore waters (Lukawska-Matuszevska 2016). Historically, the combination of alkalinity and pH has been used to estimate  $\text{CO}_2$  partial pressure ( $p\text{CO}_2$ ) in inland waters (Butman and Raymond 2011). However, several studies pointed out that this type of calculation may overestimate  $p\text{CO}_2$  because the  $\text{CO}_2$  system speciation calculations assume that the major components of alkalinity are the carbonate species (Abril et al. 2015; Hunt et al. 2011; Nydahl et al. 2017).

Given its wide presence in estuarine and coastal waters, it is desirable to explore the significance of organic alkalinity in buffering against pH change, and whether such buffer would facilitate atmospheric  $\text{CO}_2$  uptake by seawater. In addition, how terrestrially derived organic alkalinity behaves in estuarine zone is also worth investigating. This work presents a MatLab®-based framework that interested readers can utilize in their own investigations.

## 2 Methods

Based on the operational definition of TA—"the number of moles of hydrogen ion equivalent to the excess of proton acceptors (bases formed from weak acids with a dissociation constant  $K \leq 10^{-4.5}$  at 25 °C and zero ionic strength) over proton donors (acids with  $K > 10^{-4.5}$ ) in 1 kg of sample" (Dickson 1981), if an organic acid has  $pK_a < 4.5$ , addition of this acid would lead to a titration of alkalinity thus decrease its value. Therefore, in this simulation, total organic acid ( $T_{HOA} = HOA + OA^-$ , i.e., the organic acid and its conjugate base, the latter being organic alkalinity) at a concentration of 0–400  $\mu\text{mol kg}^{-1}$  (in 100  $\mu\text{mol kg}^{-1}$  increment) with the  $pK_a$  value ranging between 4.5 and 10.0 and pH ranging between 7.0 and 8.5 are chosen. The 400  $\mu\text{mol kg}^{-1}$  upper limit is arbitrarily decided as algal culture can have 400–800  $\mu\text{mol kg}^{-1}$  organic base while coastal seawater has been observed to have up to 200  $\mu\text{mol kg}^{-1}$  organic base (Hernández-Ayon et al. 2007). The simulated  $pK_a$  range includes the vast majority of natural  $pK_a$  values found in natural waters (Table 1, the discussion on organic acid with  $pK_a < 4.5$  can be found in Sect. 4.6). The pH range for the simulation encompasses the majority of natural seawater pH values including those highly productive coastal waters (Hofmann et al. 2011). The combination of  $T_{HOA}$  concentration,  $pK_a$ , and pH should generate reasonable concentration ranges of organic alkalinity ( $OA^-$ ) (Table 1). For the sake of simplicity, here a single organic acid with varying  $pK_a$  value is used in the calculations, but the readers can add any number of the acids in their buffer calculations by modifying the supplied MatLab script (Supplementary Material) with predetermined acid dissociation constants. Similarly, nutrient influence (ammonia, phosphate, and silicate) can also be examined but is not discussed here. In this simulation, two forms of organic acid addition are considered. First, organic acid with  $4.5 < pK_a \leq 10.0$  is added into seawater in the molecular form (i.e., HOA) with no change to TA (Ko et al. 2016).

**Table 1** Literature reported organic alkalinity concentrations and dissociation constants  $pK_a$

Environment	Org-A ( $\mu\text{M}$ ) <sup>a</sup>	$pK_a$	References
Phytoplankton culture	30–60	–	Kim and Lee (2009)
Phytoplankton culture	15–40	4.4–4.9 and 6.1–6.9 <sup>b</sup>	Ko et al. (2016)
Phytoplankton culture	5–20	4.0, 9.1 <sup>b</sup>	Muller and Bleie (2008)
Phytoplankton culture	200–800	5–7 <sup>c</sup>	Hernández-Ayon et al. (2007)
Coastal	22–58	5.86–7.53 <sup>c</sup>	Kuliński et al. (2014) and Ulfbo et al. (2015)
Coastal	$\leq 15$	–	Ko et al. (2016)
Estuarine and coastal	14–190	–	Hernández-Ayon et al. (2007)
Estuarine and coastal	0–56	7.27 <sup>c</sup>	Hammer et al. (2017)
Estuarine	16–34	–	Yang et al. (2015)
River	15–56	–	Wang et al. (2013)
River and Estuarine	$\sim 10$ –100 <sup>d</sup>	4.46–10 <sup>d</sup>	Cai et al. (1998)

<sup>a</sup>All organic alkalinity concentrations except those in Cai et al. (1998) were calculated using measured TA minus that calculated using DIC and pH (or  $p\text{CO}_2$ , Ulfbo et al. 2015)

<sup>b</sup> $pK_a$  values were obtained via NaOH back titration and curve fitting

<sup>c</sup> $pK_a$  values were obtained via titration curve modeling

<sup>d</sup>Organic alkalinity was analyzed using NaOH back titration;  $pK_a$  values were obtained via titration curve fitting

Second, a conjugate base of HOA is added into seawater in the ionic form (i.e.,  $\text{OA}^-$ ) along with a cation ( $\text{M}^{n+}$ ) to maintain charge balance, resulting in a net increase in TA. It is noted that even though this simulation uses the term “organic acid”, conceptually this acid can be either an organic or a mineral acid. Therefore, the results of the simulation should apply to any acid or its conjugate base addition within the defined  $pK_a$  range, despite the fact that there are only a few known inorganic acids (mostly of inorganic nutrients) that have  $pK_a$  values within this range under oxic conditions (e.g., Millero 2001).

The initial simulation condition includes  $\text{TA} = 2350 \mu\text{mol kg}^{-1}$  and  $p\text{CO}_2 = 400 \mu\text{atm}$  at air-seawater equilibrium. At salinity 35 and temperature 15 °C, the equilibrium DIC concentration is  $2124 \mu\text{mol kg}^{-1}$ , which is calculated using the carbonic acid dissociation constants ( $K_1$  and  $K_2$ ) reported in Mehrbach et al. (1973) and refit by Dickson and Millero (1987), the bisulfate dissociation constant reported in Dickson et al. (1990), and the total boron concentration in Uppström (1974). Even though bisulfate is considered as negative alkalinity in the TA definition (Dickson 1981), the values are negligible at the simulation pH range (i.e.,  $0.019 \mu\text{mol kg}^{-1}$  at pH 7.0 and  $<0.001 \mu\text{mol kg}^{-1}$  at pH 8.5, note pH on the free scale ( $\text{pH}_F$ ) is used here), so this negative contribution to TA is not included in the simulations. Note the refitted constants presented in Dickson and Millero (1987) are on the seawater scale (SWS), and the MatLab version of the program CO2SYS (Ver. 1.1) converts these constants to be based on the free scale (Line 1806–1807 in the function FindpHOnAllScales, van Heuven et al. 2011). All constants at the simulation temperature and salinity are taken from the CO2SYS program.

To calculate the perturbations of organic acid to seawater, two scenarios are simulated for both HOA and  $\text{OA}^-$  additions. Both changes in  $p\text{CO}_2$  under a closed-system condition (i.e., constant DIC) and the expected DIC concentration changes to “restore” the perturbed seawater back to air-seawater equilibrium ( $p\text{CO}_2 = 400 \mu\text{atm}$ ) under an open-system condition are calculated. These two scenarios are included to reflect seawater that is not subject to air-sea gas exchange (below the mixed layer) and that freely exchanges with the atmosphere. For each  $T_{\text{HOA}}$  level ( $0$ – $400 \mu\text{mol kg}^{-1}$ ), a two-dimensional matrix ( $\text{pH}$  vs.  $pK_a$ ) is calculated using the MatLab scripts in Supplementary Material (Organic\_Alkalinity\_HOA.m and Organic\_Alkalinity\_OA.m). Next, for each  $pK_a$  value, a search for the speciation solution after the HOA or  $\text{OA}^-$  addition for a closed system with fixed DIC ( $p\text{CO}_2$ ,  $\beta_{\text{DIC}}$ , and organic alkalinity or  $[\text{OA}^-]$ ) and for an open system that allows air-sea re-equilibration at  $p\text{CO}_2 = 400 \mu\text{atm}$  (DIC,  $\beta_{\text{DIC}}$ , and  $[\text{OA}^-]$ ) is done using the MatLab command “*interp1*” and the “*pchip*” interpolating algorithm (i.e., shape-preserving piecewise cubic interpolation). Using this approach, complex analytical solution of the multiple nonlinear equations of the acid–base buffer system can be avoided.

To evaluate the effect of organic alkalinity on buffer capacity changes, an extended buffer factor based on Egleston et al. (2010) was obtained:

$$\beta_{\text{DIC}} = \left( \frac{\partial \ln ([\text{H}^+])}{\partial \text{DIC}} \right)^{-1} = \frac{\text{DIC} \times S - \text{TA}_C^2}{\text{TA}_C} \quad (1)$$

In Eq. (1)  $\text{TA}_C$  is carbonate alkalinity,  $S = [\text{HCO}_3^-] + 4[\text{CO}_3^{2-}] + \frac{[\text{B(OH)}_4^-][\text{H}^+]}{K_B + [\text{H}^+]} + \frac{[\text{OA}^-][\text{H}^+]}{K_{\text{HOA}} + [\text{H}^+]} + [\text{H}^+] + [\text{OH}^-]$  (see Supplementary Material for the detailed derivation steps), in which  $K_B$  and  $K_{\text{HOA}}$  are dissociation constants of boric and organic acids, respectively.

$\beta_{\text{DIC}}$  reflects the change of  $[\text{H}^+]$  (or pH) in response to the addition of  $\text{CO}_2$ . Lower values indicate less buffer and higher values indicate stronger buffer, although see below (Sect. 4.4) for a discussion on high  $\beta_{\text{DIC}}$  values at higher  $p\text{CO}_2$  and low pH conditions.

Finally, in addition to calculating buffer effect of organic acid on the seawater endmember, the influence of organic alkalinity in estuarine mixing zone using the same seawater but without organic alkalinity and a river endmember is also evaluated. River water has varying levels of weathering products due to many factors including drainage basin mineralogy, river hydrology, and biogeochemical reactions. For simplicity, a DIC concentration of  $1050 \mu\text{mol kg}^{-1}$  and a TA value of  $1000 \mu\text{mol kg}^{-1}$  are selected for this simulation. These values are bracketed by rivers with high levels of weathering products (for example, the Mississippi River), and those that have little (for example, Amazon) (Hu and Cai 2013). Similar to the method above, multiple river  $T_{\text{HOA}}$  levels (at constant river alkalinity) are used in the mixing simulations. As little is known regarding the salinity-dependent dissociation constant of natural organic acids, here simulations using only two fixed “boundary”  $pK_a$  values are presented (4.50 and 8.20, the latter being the calculated  $pK_a$  that provides the greatest buffer to seawater, see Sect. 3.2) across the estuarine mixing zone. The readers can use the supplied MatLab scripts to examine other  $pK_a$  values found in natural organic acids and their respective concentrations (see Table 1), as well as rivers with different inorganic carbon system parameters. Similar to the simulations on the seawater-only cases above, both closed- and open-systems are also considered.

### 3 Results

#### 3.1 Changes to $p\text{CO}_2$ , pH, and DIC Under Closed- and Open-System Conditions due to Organic Acid Addition

If DIC concentration is maintained after the addition of HOA under a closed-system condition, seawater  $p\text{CO}_2$  would be higher than the starting conditions (400  $\mu\text{atm}$ , Fig. 1a). In contrast, if  $\text{OA}^-$  is added into the system (with accompanying cations),  $p\text{CO}_2$  would decrease (Fig. 1b). Furthermore, both  $pK_a$  and  $T_{\text{HOA}}$  determine the magnitude of  $p\text{CO}_2$  increase or decrease. Generally, at fixed level of  $T_{\text{HOA}}$ ,  $p\text{CO}_2$  is higher following HOA addition at a lower  $pK_a$  (i.e., stronger acid leads to greater  $p\text{CO}_2$  increase, Fig. 1a). For  $\text{OA}^-$  addition however,  $p\text{CO}_2$  is lower at a higher  $pK_a$  (i.e., stronger conjugate base of a weaker acid leads to greater  $p\text{CO}_2$  decline, Fig. 1b). On the other hand, higher  $T_{\text{HOA}}$  concentration leads to higher  $p\text{CO}_2$  (HOA) or lower  $p\text{CO}_2$  ( $\text{OA}^-$ ) at fixed  $pK_a$  (Fig. 1a, b). Because the addition of HOA (without changing TA) increases  $p\text{CO}_2$ , one would expect to see  $\text{CO}_2$  degassing if this perturbed seawater is exposed to the air, which would result in a decrease in DIC concentration compared to the original value (excess DIC in Fig. 1c). Conversely, an addition of  $\text{OA}^-$  increases TA but does not change DIC, resulting in  $p\text{CO}_2$  decrease. Subsequent  $\text{CO}_2$  uptake would result in DIC increase after air-seawater re-equilibration under the open-system condition (DIC deficiency in Fig. 1d). From the calculation results, as much as  $339 \mu\text{mol kg}^{-1}$  DIC would need to be degassed (from the initial  $2124 \mu\text{mol kg}^{-1}$ ) or  $334 \mu\text{mol kg}^{-1}$  DIC needs to be taken up from the atmosphere to restore seawater  $p\text{CO}_2$  back to the starting condition when  $T_{\text{HOA}} = 400 \mu\text{mol kg}^{-1}$  (Fig. 1c, d) following HOA addition or  $\text{OA}^-$  addition, respectively.

As expected, organic acid with lower  $pK_a$  (stronger acid) would have more complete dissociation hence higher levels of  $\text{OA}^-$  (within  $\text{TA} = 2350 \mu\text{mol kg}^{-1}$ , Fig. 1e). Because

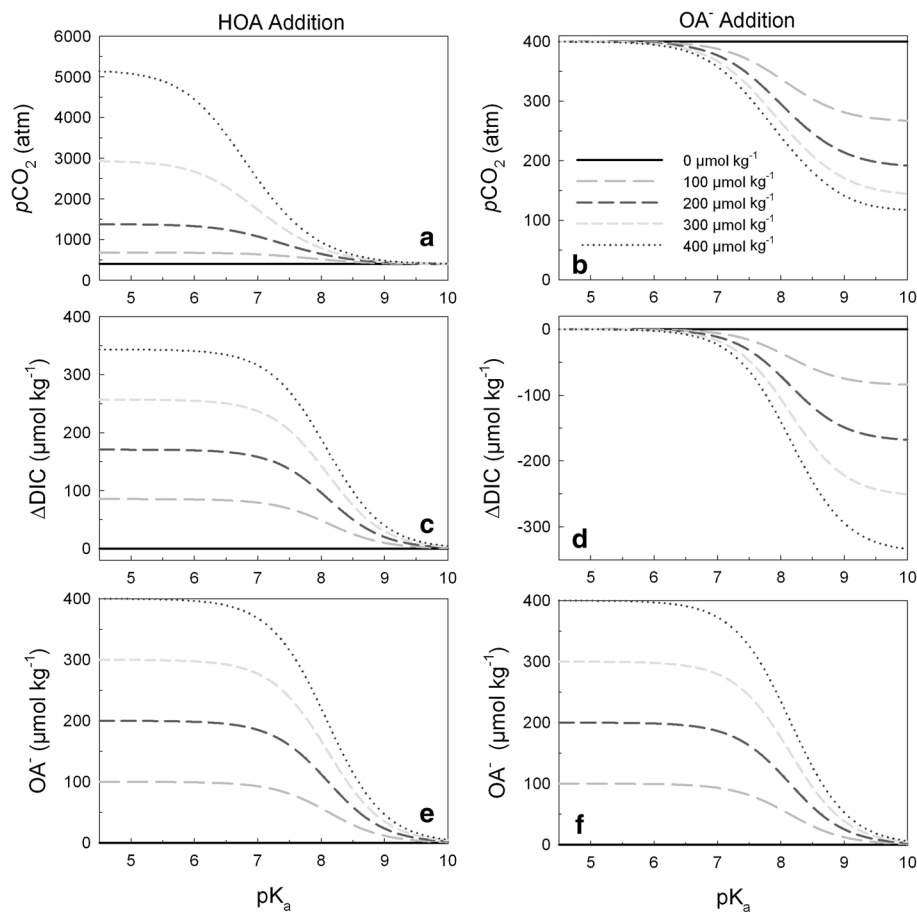


**Fig. 1** Seawater  $p\text{CO}_2$  after the addition of organic acid (HOA, **a**) or organic base ( $\text{OA}^-$ , **b**) at constant  $\text{DIC} = 2123.6 \mu\text{mol kg}^{-1}$  in a closed system. Expected DIC loss due to  $\text{CO}_2$  degassing after HOA addition (**c**, excess DIC) and  $\text{CO}_2$  uptake (**d**, DIC deficiency) after the perturbed seawater reach equilibrium with atmosphere at 400  $\mu\text{atm}$  (open system). Concentrations of  $\text{OA}^-$  at  $p\text{CO}_2 = 400 \mu\text{atm}$  for both HOA and  $\text{OA}^-$  addition (**e**, **f**). Simulation initial condition,  $\text{TA} = 2350 \mu\text{mol kg}^{-1}$ ,  $S = 35$ ,  $T = 15^\circ\text{C}$ . The legend shows total concentrations of organic acid (undissociated HOA and its conjugate base  $\text{OA}^-$ , or  $T_{\text{HOA}}$ ). Note that the panels **e** and **f** show similar patterns because the differences in  $[\text{OA}^-]$  at each  $T_{\text{HOA}}$  concentration across the simulated  $pK_a$  range are small relative to the scale of the y-axis

of their overall higher pH conditions for each level of simulated  $T_{\text{HOA}}$  addition (Fig. 2a, b), final  $[\text{OA}^-]$  concentrations following the  $\text{OA}^-$  addition in the open system (Fig. 1f) are slightly higher (by up to  $11 \mu\text{mol kg}^{-1}$ ) than those in the scenarios with HOA addition (Fig. 1e) at the same  $pK_a$ .

### 3.2 Buffer Capacity Under Closed- and Open-System Conditions due to Organic Acid Addition

Contrary to the readily apparent "acidification" effect caused by either HOA addition in seawater (i.e., pH decreases for all levels of organic acid addition, Fig. 2a) or the "basification"

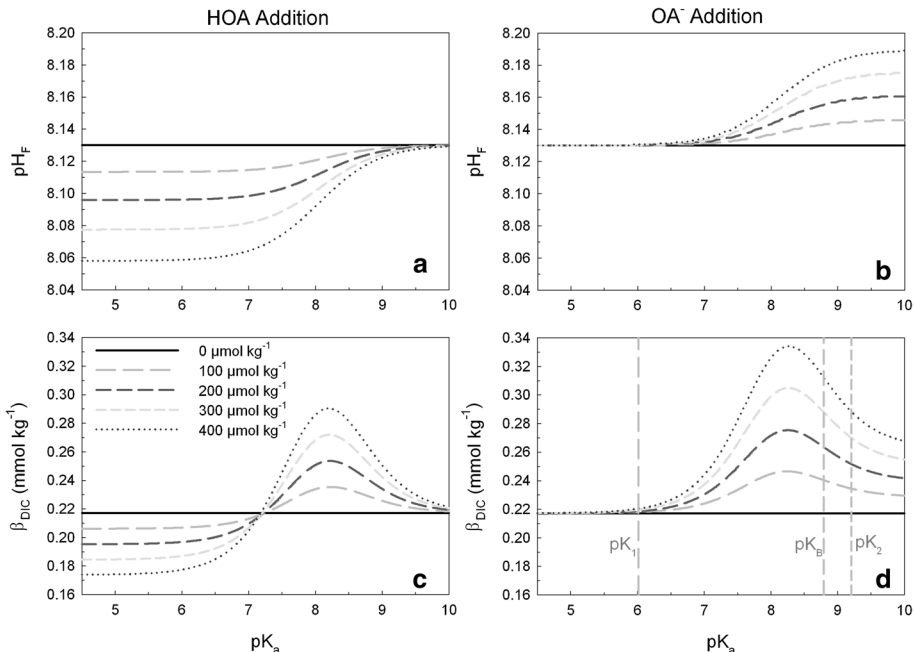


**Fig. 2** Seawater pH (a, b) and  $\beta_{\text{DIC}}$  (c, d) following HOA (or  $\text{OA}^-$ ) addition and subsequent degassing (or  $\text{CO}_2$  uptake) in an open system. All values are calculated at  $p\text{CO}_2=400$   $\mu\text{atm}$ . Simulation condition,  $\text{TA}=2350$   $\mu\text{mol kg}^{-1}$ ,  $S=35$ ,  $T=15$   $^\circ\text{C}$

effect caused by  $\text{OA}^-$  addition (i.e., pH increases, Fig. 2b), after the perturbed water is re-equilibrated with the same atmosphere  $p\text{CO}_2$  of 400  $\mu\text{atm}$ , buffer capacity  $\beta_{\text{DIC}}$  exhibits rather complex behaviors (Fig. 2c, d). For the HOA addition scenario, if  $pK_a$  of organic acid is lower than a certain threshold (i.e.,  $\sim 7.15$  for the model seawater at  $T=15$   $^\circ\text{C}$  and  $S=35$ , Fig. 2c),  $\beta_{\text{DIC}}$  of organic acid-perturbed seawater is lower than that of the original seawater (note the intercepts between the various  $T_{\text{HOA}}$  levels and the unperturbed seawater are close but not exactly the same, Fig. 2c). However, when  $pK_a$  is greater than this threshold, organic acid-perturbed seawater appears to have greater buffer capacity than that of the original seawater, i.e.,  $[\text{H}^+]$  is less sensitive to DIC addition than the unperturbed seawater (see  $\beta_{\text{DIC}}$  definition in Eq. 1), despite that this perturbed seawater has lower pH than the unperturbed one (Fig. 2a). The maximum buffer appears when  $pK_a=8.20$  at the simulation condition (Fig. 2c). For the  $\text{OA}^-$  addition scenario,  $\beta_{\text{DIC}}$  increases in all cases. Similar to HOA addition, the highest buffer also appears at the higher  $pK_a$  range, here 8.25 (Fig. 2d), slightly higher than that for HOA addition (Fig. 2c).

### 3.3 Changes in pH of Maximum $\beta_{\text{DIC}}$ due to Organic Acid Addition

For a monoprotic acid (HOA), the maximum buffer occurs at its  $pK_a$  value as the concentrations of the undissociated acid (HOA) and its conjugate base ( $\text{OA}^-$ ) are the same, i.e., the equivalence point, where  $\text{pH}=pK_a$  (provided that the acid concentration is not too low, otherwise water dissociation would become more important). Whereas for a diprotic acid ( $\text{H}_2\text{OA}$ ), maximum buffer occurs at two equivalence points, i.e.,  $[\text{H}_2\text{OA}]=[\text{HOA}^-]$

( $\text{pH} = pK_{a,1}$ , i.e., the first dissociation constant) and  $[\text{HOA}^-] = [\text{OA}^{2-}]$  ( $\text{pH} = pK_{a,2}$ , i.e., the second dissociation constant) (Stumm and Morgan 1995). Addition of other acid–base pairs into the diprotic acid solution would alter the pH where the buffer maxima (as well as minima) appear. For example, in the seawater used in this simulation (i.e.,  $\text{TA} = 2350 \mu\text{mol kg}^{-1}$ ,  $S = 35$ ,  $T = 15^\circ\text{C}$ ),  $pK_1 = 6.02$ ,  $pK_2 = 9.20$  (again, these values are on the free pH scale), the buffer maximum that corresponds to  $[\text{CO}_3^{2-}] = [\text{HCO}_3^-]$  would have been  $\text{pH} = pK_2 = 9.20$  provided there are no other acid–base pairs ( $\text{pH} = pK_1$  is the other maximum buffer at lower pH, Fig. 3). Although because of the presence of borate, maximum  $\beta_{\text{DIC}}$  appears at lower pH (8.82) than  $pK_2$  (note  $pK_B = 8.79$ ). The same applies to the adjacent minimum  $\beta_{\text{DIC}}$  when  $\text{DIC} = \text{TA}$ , i.e., instead of  $\text{pH} = (pK_1 + pK_2)/2 = 7.61$ , the minimum  $\beta_{\text{DIC}}$  appears at pH 7.58 (Egleston et al. 2010; Hu and Cai 2013) (Fig. 3). Assuming that  $pK_a$  of HOA is 8.20, the maximum buffer occurs as pH 8.66 when HOA is added (or pH 8.69 if  $\text{OA}^-$  is added), which is a further decrease from the organic alkalinity-free seawater (pH 8.82, see above) (Fig. 3). Note that  $\beta_{\text{DIC}}$  at the assumed air  $p\text{CO}_2$  condition (400  $\mu\text{atm}$ ) is not at its maximum in the simulated pH range and will decrease further with continued ocean acidification (Fig. 3).

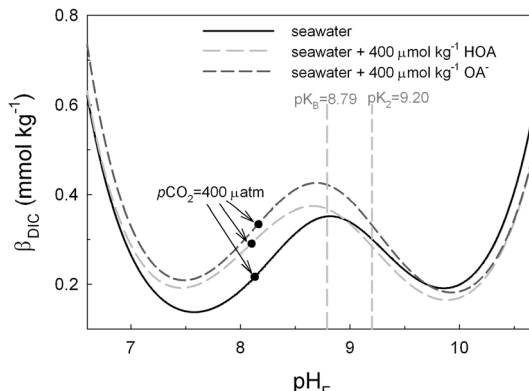
### 3.4 Influence of Organic Alkalinity in Estuarine Mixing Zone

At the given river endmember DIC and TA values and assuming that the river water is organic free,  $p\text{CO}_2$  is 1147  $\mu\text{atm}$  at  $15^\circ\text{C}$  using the carbonate dissociation constants in Millero (1979). This  $p\text{CO}_2$  level is realistic (i.e., higher than the atmospheric  $p\text{CO}_2$ ) and falls within the natural river  $p\text{CO}_2$  range (Butman and Raymond 2011).

Clearly, both  $pK_a$  value and organic acid concentration play important roles in the speciation of the buffer system in the estuarine zone (Figs. 4, 5). Compared to the zero  $T_{\text{HOA}}$  condition (the dark red curves in Figs. 4, 5), the presence of organic acid–base in river water always increases  $p\text{CO}_2$  and decrease  $\text{pH}_F$  in the mixing zone for the closed system (Fig. 4a, b), and upon complete air–water equilibration (open system), DIC decreases due to  $\text{CO}_2$  degassing (Fig. 5a) and pH is nevertheless still lower than the mixing between zero  $T_{\text{HOA}}$  condition (Fig. 5b). This result is similar to the situation where HOA is added into seawater (Fig. 2a).

Based on the simulation, stronger organic acid leads to more acidified estuarine water (solid curves in Figs. 4a, b and 5b). Furthermore, in the closed system the concentration of the conjugate base ( $\text{OA}^-$ ) of the stronger organic acid ( $pK_a = 4.5$ ) exhibits a close to linear

**Fig. 3** Simulated  $\beta_{\text{DIC}}$  in seawater, seawater +  $400 \mu\text{mol kg}^{-1}$  HOA, and seawater +  $400 \mu\text{mol kg}^{-1}$   $\text{OA}^-$ . Simulation initial condition,  $\text{TA} = 2350 \mu\text{mol kg}^{-1}$ ,  $S = 35$ ,  $T = 15^\circ\text{C}$ , HOA  $pK_a = 8.20$ . The three closed circles represent  $p\text{CO}_2 = 400 \mu\text{atm}$  for the three simulations. Maximum  $\beta_{\text{DIC}}$  appears at pH 8.82, 8.66, and 8.69 for these three simulations, respectively



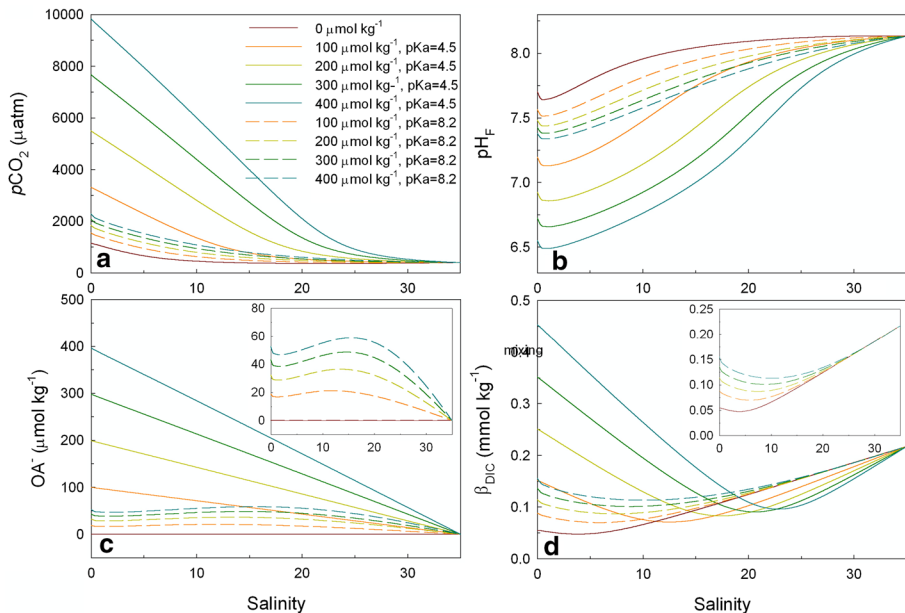


**Fig. 4**  $p\text{CO}_2$  (a),  $\text{pH}_F$  (b),  $[\text{OA}^-]$  (c) and  $\beta_{\text{DIC}}$  (d) as a function of salinity in the river-ocean mixing zone in a closed system. The inserts in panels c and d are blown-up views of results calculated with  $pK_a=8.20$ . The river endmember has  $\text{DIC}=1050 \mu\text{mol kg}^{-1}$ ,  $\text{TA}=1000 \mu\text{mol kg}^{-1}$  with various levels of total organic acid (0, 100, 200, 300, 400  $\mu\text{mol kg}^{-1}$ ). The ocean endmember is set to be the same as that in seawater simulation with zero organic acid, i.e.,  $\text{TA}=2350 \mu\text{mol kg}^{-1}$ ,  $p\text{CO}_2=400 \mu\text{atm}$ ,  $S=35$ ,  $T=15^\circ\text{C}$ . Conservative mixing of TA and DIC is assumed in this calculation. See text for details

relationship with salinity (Fig. 4c), while the weaker organic acid ( $pK_a=8.2$ ) yield a mid-salinity maximum in  $[\text{OA}^-]$  (the insert in Fig. 4c). In the open system, such distinction is less clear as  $[\text{OA}^-]$  shows a nearly linear relationship with salinity across most of the mixing zone (Fig. 5c).

In the close system,  $\beta_{\text{DIC}}$  of the two organic acids both show a mid-salinity  $\beta_{\text{DIC}}$  minimum, and the salinity at which the  $\beta_{\text{DIC}}$  minimum appears is lower for the weaker acid (dashed curves in Fig. 4d). Despite this commonality, the weaker organic acid increased  $\beta_{\text{DIC}}$  value across all salinity range compared to the no zero  $T_{\text{HOA}}$  condition (the dark red curve), while the stronger organic acid depresses the  $\beta_{\text{DIC}}$  value at mid to high salinity relative to the zero  $T_{\text{HOA}}$  condition, although at lower salinities  $\beta_{\text{DIC}}$  values are higher (Fig. 4d). In the open system however, the stronger acid depresses  $\beta_{\text{DIC}}$  across all salinity range while the weaker acid elevates  $\beta_{\text{DIC}}$  slightly (Fig. 5d) relative to the zero  $T_{\text{HOA}}$  river condition. This again is similar to HOA addition into seawater and  $\beta_{\text{DIC}}$  is elevated for organic acid with high  $pK_a$  values (Fig. 2c).

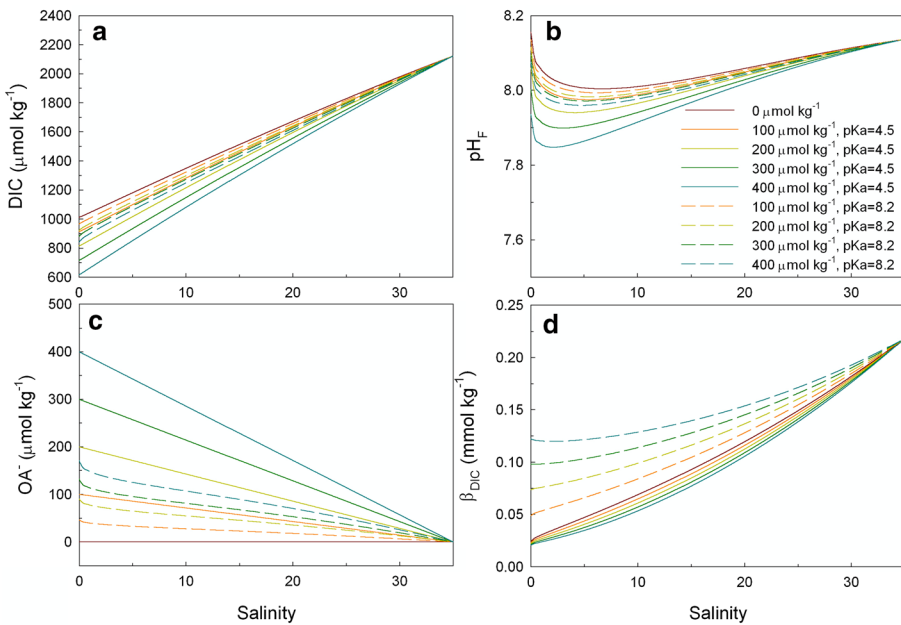


**Fig. 5**  $p\text{CO}_2$  (a),  $\text{pH}_F$  (b),  $[\text{OA}^-]$  (c) and  $\beta_{\text{DIC}}$  (d) as a function of salinity in the river-ocean mixing zone in an open system. The river and ocean endmember compositions are the same as those in Fig. 4. Since the entire mixing zone is assumed to be an open system,  $p\text{CO}_2$  across the salinity gradient is uniformly 400  $\mu\text{atm}$

## 4 Discussion

### 4.1 Controls on $pK_a$ that Corresponds to Maximum $\beta_{\text{DIC}}$

Not only is the seawater  $\beta_{\text{DIC}}$  maximum affected by the form of organic acid added (i.e., HOA and  $\text{OA}^-$ ), but  $pK_a$  that corresponds to the maximum  $\beta_{\text{DIC}}$  is also a function of the equilibrium  $p\text{CO}_2$ . For both HOA and  $\text{OA}^-$  additions,  $pK_a$  that corresponds to maximum  $\beta_{\text{DIC}}$  (Fig. 2c, d) decreases with increasing  $p\text{CO}_2$ , the same also applies to the threshold  $pK_a$  (defined here as the “transition  $pK_a$ ,” Fig. 6), i.e., the intercept  $pK_a$  value between the perturbed and unperturbed seawater for HOA addition (see Fig. 2c). The physical meaning of these shifts is that stronger organic acid (lower  $pK_a$ ) and its conjugate base play a more important role controlling seawater buffer capacity at higher  $p\text{CO}_2$  levels. Compared to the equilibrium  $p\text{CO}_2$  control, temperature and salinity have less influence on the value of  $pK_a$  at the  $\beta_{\text{DIC}}$  maximum. For example, at  $S=35$  and  $25\text{ }^\circ\text{C}$  with  $p\text{CO}_2=400\text{ }\mu\text{atm}$  (TA is  $2350\text{ }\mu\text{mol kg}^{-1}$  for HOA addition or  $2750\text{ }\mu\text{mol kg}^{-1}$  with  $\text{OA}^-$  addition) and  $400\text{ }\mu\text{mol kg}^{-1}$   $T_{\text{HOA}}$  concentration,  $pK_a$  at maximum  $\beta_{\text{DIC}}$  is only greater by 0.05 than the value at  $15\text{ }^\circ\text{C}$ , when all other conditions are kept the same (Figs. S1 and S2). Similarly, changing salinity from 35 to 20 while maintaining the same TA (for simplicity assuming river TA and ocean TA equal each other),  $pK_a$  only increases by 0.02 (Figs. S1 and S2). These differences indicate that weaker organic acid–base pair exerts stronger control at higher temperature and lower salinity, although the changes are smaller than the changes caused by seawater  $p\text{CO}_2$  change (Fig. 6). On the other hand, fluctuating seawater  $p\text{CO}_2$

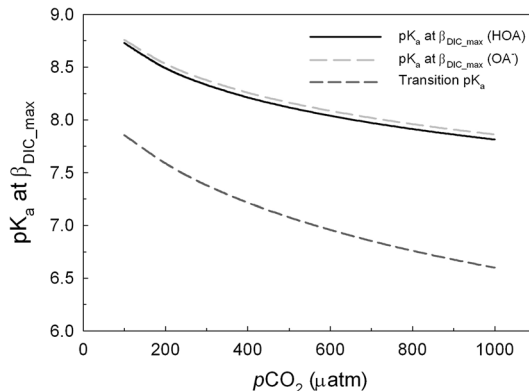


**Fig. 6**  $pK_a$  values that correspond maximum  $\beta_{DIC}$  for HOA addition (solid curve),  $OA^-$  addition (dashed grey curve), and the threshold condition (cf. Fig. 2c, dashed black curve) as a function of equilibrating  $pCO_2$ . Each curve represents an average of four  $T_{HOA}$  scenarios ( $100 \mu\text{mol kg}^{-1}$ ,  $200 \mu\text{mol kg}^{-1}$ ,  $300 \mu\text{mol kg}^{-1}$ , and  $400 \mu\text{mol kg}^{-1}$ ). Average standard deviations of these scenarios are 0.01 (both HOA and  $OA^-$  addition) and 0.03 (the threshold value) and are not shown in the figure. Simulation initial condition, TA =  $2350 \mu\text{mol kg}^{-1}$ ,  $S = 35$ ,  $T = 15^\circ\text{C}$

under natural conditions means that not a single organic acid may provide the maximum amount of buffer, but a collection of these acids that have relatively high  $pK_a$  values would be responsible for this buffer effect. It is also worth noting that other buffer factors should exhibit similar behaviors as they all show similar patterns in the seawater system (Egleston et al. 2010).

#### 4.2 Effect of Organic Alkalinity Addition on Seawater Uptake of Atmospheric $\text{CO}_2$

Following HOA addition,  $pCO_2$  increase and  $\text{CO}_2$  degassing would occur (Fig. 1c). This  $\text{CO}_2$  loss in an open system is expected, as HOA addition into a seawater is essentially the same as ocean acidification or adding any other acid. However, the dissociation of the organic acid produces its corresponding conjugate base,  $OA^-$ , rather than bicarbonate or carbonate (the conjugate bases for carbonic acid); hence,  $OA^-$  replaces these two carbonate species, causing overall DIC decrease due to  $\text{CO}_2$  loss (Fig. 1c).

Using the literature reported  $pK_a$  values found in various seawater media (Table 1), phytoplankton culture or other environments may produce relatively strong organic acids in the form of HOA, as most calculated  $pK_a$  values are less than 7.15 (i.e., the transition  $pK_a$  in Fig. 2c). Hypothetically, if the perturbed seawater following the addition of these organic acids is equilibrated with the atmosphere, then it has lower buffer capacity than the unperturbed seawater.

In contrast to net HOA addition, if  $OA^-$  is added into seawater in a net sense,  $\text{CO}_2$  uptake would occur (Fig. 1d). In this scenario, a weak base ( $OA^-$ ) combines with proton to form HOA. This process leads to an increase in pH (not shown) and decrease in  $pCO_2$  (Fig. 1b) in a closed system. However, before answering the question whether net  $OA^-$  addition is a process that helps seawater take up  $\text{CO}_2$ , it is worth exploring whether organic alkalinity represents a net addition to the inorganic acid–base system in seawater and what the fates are for organic molecules in the seawater.

### 4.3 Is Organic Alkalinity an "Extra" Source of Seawater Alkalinity in Nature?

In the literature, there are conflicting views on whether organic alkalinity contributes to net TA increases in seawater. First, Kim et al. (2006) suggested that phytoplankton cells contribute to TA when particulate organic carbon level is greater than  $200 \text{ }\mu\text{mol kg}^{-1}$  (the cells have alkalinity of  $3\text{--}5 \text{ }\mu\text{mol kg}^{-1}$ ), and bacteria contribute  $1\text{--}6 \text{ }\mu\text{mol kg}^{-1}$ . However, Hernández-Ayon et al. (2007) compared filtered and unfiltered phytoplankton culture and did not observe significant difference within a  $5 \text{ }\mu\text{mol kg}^{-1}$  uncertainty. It is worth noting that the later study does not necessarily invalidate the earlier findings as the two studies have different levels of analytical precision, i.e.,  $\pm 1 \text{ }\mu\text{mol kg}^{-1}$  in Kim et al. (2006) and  $\pm 4\text{--}5 \text{ }\mu\text{mol kg}^{-1}$  in Hernández-Ayon et al. (2007). Nevertheless, the contribution from live cells appears to have a much smaller influence on TA compared to organic alkalinity discussed below.

Kim and Lee (2009) used phytoplankton culture under high nutrient conditions to study the potential organic alkalinity production. These authors used cultured media, in which TA increase exceeds the extent of nitrate consumption with a  $-(\Delta\text{TA}/\Delta\text{NO}_3)$  ratio of 1.11–1.45, indicating “excess” alkalinity production (11–45% more than the nitrate taken up by the phytoplankton) that cannot be explained by simple reaction stoichiometry of anion uptake, because one unit of nitrate utilization theoretically produces one unit of alkalinity. In these phytoplankton cultures ( $10^4\text{--}10^5 \text{ cell ml}^{-1}$ ), organic alkalinity ranges  $30\text{--}60 \text{ }\mu\text{mol kg}^{-1}$  with similar increase in the dissolved organic carbon (DOC) concentrations. However, in a follow-up study that investigated phytoplankton cultures by the same group (Ko et al. 2016), organic acid addition into seawater was not found to influence TA. These authors interpreted that the weak acid addition only shifts acid–base equilibria and not total amount of acid neutralizing capacity, making it essentially equivalent to HOA addition to seawater as discussed above.

Despite that both HOA and  $\text{OA}^-$  additions are considered in the perturbation simulations, to add organic alkalinity in a net sense (i.e., increase TA), the anion  $\text{OA}^-$  needs to enter the seawater along with cation(s) to maintain a charge balance. To achieve this, organic acids in the molecular form produced through biogeochemical reactions need to react with minerals to produce the conjugate base anion along with cations from mineral dissolution (for example carbonate or silicate) (e.g., Lundegard and Land 1989; Welch and Ullman 1993), although this type of reaction is far more complex than a simple dissolution of minerals. Nevertheless, it is likely that environments with significant presence of minerals (such as wetlands, shallow estuaries, and coastal areas) that allow organic acid–mineral reactions may have the capacity to increase total alkalinity in a net sense.

### 4.4 Organic Alkalinity and Its Buffer Effect in the Estuarine Zone

When river water carries organic acid and enters estuarine mixing zone, the presence of organic acid and its conjugate base not only shifts the acid–base equilibria across the salinity gradient, but also the buffer behavior of the estuarine water, compared with the scenario that river water has only carbonate alkalinity (i.e., the zero- $T_{\text{HOA}}$  river, the dark red curves in Figs. 4, 5). Clearly, not accounting for the presence of organic alkalinity would underestimate  $p\text{CO}_2$  if using TA and DIC as the input pair for the  $\text{CO}_2$  system speciation calculations (Fig. 4a), regardless of the dissociation constant. Similarly, using pH and TA as the input pair without considering the contribution of organic alkalinity (Fig. 4c)

would overestimate  $p\text{CO}_2$  as what previous studies have shown (Abril et al. 2015; Hunt et al. 2011; Nydahl et al. 2017).

Replacing carbonate alkalinity with organic alkalinity (i.e., maintain the constant alkalinity level) alters buffer capacity of estuarine water (Figs. 4d, 5d). It is clear that organic acid with lower  $pK_a$  causes greater deviation in  $\beta_{\text{DIC}}$  compared with mixing between zero- $T_{\text{HOA}}$  river water and seawater in a closed system (Fig. 4d). At higher salinity,  $\beta_{\text{DIC}}$  values are lower than values from this mixing scenario, and at lower salinity  $\beta_{\text{DIC}}$  increases (Fig. 4d). This reversal in  $\beta_{\text{DIC}}$  values is because carbonate and borate ion concentrations are very low at high  $p\text{CO}_2$  and low pH conditions; hence, the buffer is provided by diluting  $\text{CO}_2$  into existing DIC (Egleston et al. 2010), while less proton concentration change would occur at given  $\text{CO}_2$  addition, yielding greater  $\beta_{\text{DIC}}$ . In other words, this increase in  $\beta_{\text{DIC}}$  with decreasing salinity does not translate to resistance to acidification by any means because water  $p\text{CO}_2$  level is already high (Fig. 4a). Instead, this high  $p\text{CO}_2$  water would acidify seawater with lower  $p\text{CO}_2$  levels upon mixing. This type of elevated  $\beta_{\text{DIC}}$  values along with high DIC and  $p\text{CO}_2$  levels were also observed in other estuarine settings (e.g., Wang et al. 2016). Similar to the seawater endmember simulation, organic acid with higher  $pK_a$  always results in elevated buffer regardless of whether the system is open or not (Figs. 4d, 5d).

As  $pK_a$  increases, all calculated  $p\text{CO}_2$ ,  $\text{pH}_F$ ,  $\text{OA}^-$ , and  $\beta_{\text{DIC}}$  values approach the results from mixing between carbonate zero- $T_{\text{HOA}}$  river water and seawater (Figs. 4d, 5d). This result is reasonable, because as the organic acid is weaker, it would play a less important role in regulating the buffer system. Using this simulation, it is clear that the effect of organic alkalinity on estuarine buffer diminishes with increasing salinity, regardless of the  $pK_a$  values.

In reality, estuarine mixing and river export to the coastal ocean occur on vastly different time scales, and depending on these time scales, various extent of degassing due to high- $\text{CO}_2$  river water discharge would occur (Borges et al. 2006; Jiang et al. 2008), to the extent that all excess DIC is lost through air–water equilibrium in an open system (Fig. 5a). Therefore, organic alkalinity in an estuarine mixing zone may be expected to behave between the two extreme scenarios, i.e., closed vs. open (Figs. 4, 5), as a function of estuarine residence time.

## 4.5 The Fate of Organic Alkalinity

In the literature, higher organic alkalinity levels are commonly found in rivers, and its contribution to TA diminishes in higher salinity waters (Cai et al. 1998; Hunt et al. 2011; Wang et al. 2013; Yao and Hu 2017), just like what the simple numerical simulations above suggest. Certainly, in reality the decrease of organic alkalinity concentration across a salinity gradient are only partially attributed to dilution, as both photochemical and microbial processes may also break down these organic molecules (e.g., Amon and Benner 1996; Fichot and Benner 2014). To the best of the author's knowledge, there is currently no study investigating the degradation of organic alkalinity on seawater acid–base chemistry.

To explore the theoretical effect of organic alkalinity degradation, it is reasonable to consider a simplistic scenario using a "model compound". The simplest organic acid–formic acid ( $\text{HCOOH}$ ) has  $pK_a$  lower than 4; thus, it is not an ideal representative for this simulation. Acetic acid ( $\text{CH}_3\text{COOH}$ , or  $\text{HAc}$ ) ( $pK_a = 4.76$  in freshwater at  $25^\circ\text{C}$ , Serjeant and Dempsey 1979) is taken as an example to illustrate the organic acid perturbation, and the conjugate base of acetic acid—acetate ( $\text{Ac}^-$ )—is used as a model species to represent

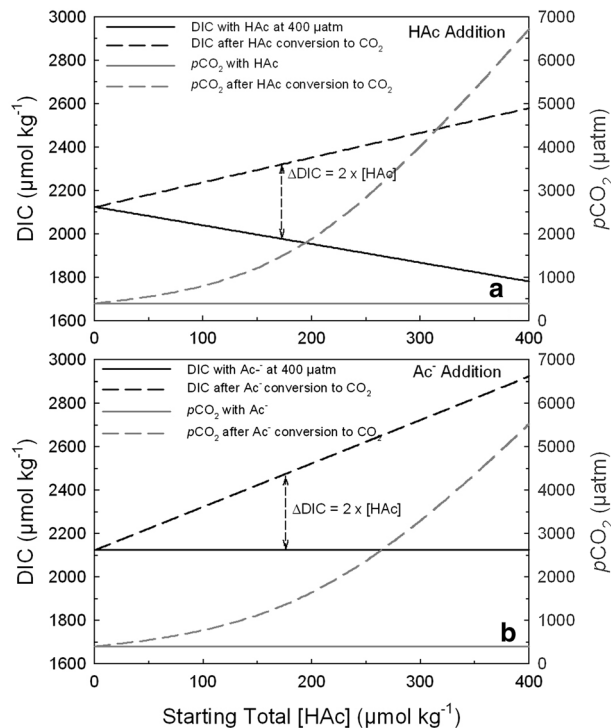
organic alkalinity. Note that  $pK_a$  decreases by  $\sim 0.15$  at seawater ionic strength (Millero 1983). Although for the sake of simplicity, the freshwater value  $pK_a$  value is used here, because even after the salting coefficient correction,  $pK_a$  would still be greater than 4.5. A complete degradation of the acetate can be represented as:



Clearly, this reaction produces DIC but does not change TA, a process equivalent to the “charge transfer” mechanism in an earlier seawater alkalinity dynamics discussion (Hu and Cai 2011). In other words, the addition of HAc into seawater and subsequent complete breakdown to  $\text{CO}_2$  has no effect on TA but leads to a net increase in DIC, while the addition of an acetate salt ( $\text{Ac}^-$ ) increases TA by the amount of acetate added, and the breakdown of acetate also increases DIC. Simulations of both HAc and  $\text{Ac}^-$  additions and final remineralization indicate that  $p\text{CO}_2$  increases for both cases (Fig. 7). Moreover, even though the final DIC concentration is higher for the  $\text{Ac}^-$  addition (due to the initial  $\text{CO}_2$  uptake in an open system after the  $\text{Ac}^-$  addition, Fig. 7b) than the addition of HAc (Fig. 7a), the  $p\text{CO}_2$  level is lower at any given amount of HAc because of higher TA level caused by the net  $\text{Ac}^-$  addition (Fig. 7). Similar to the acetate addition, it is common knowledge among the saltwater aquarium hobbyists that vinegar and a “limewater” (i.e.,  $\text{Ca}(\text{OH})_2$  solution) can be used together to increase alkalinity and calcium levels in tanks that host hard corals, a process that is equivalent to the simulation of  $\text{Ac}^-$  addition here.

In natural waters, humic substances represent the largest dissolved organic matter fraction, and carboxyl and phenolic hydroxyl groups in the complex humic “molecules” give rise to their acidity (Perdue et al. 1980). Based on the above discussion, it is likely that

**Fig. 7** Two hypothetical scenarios of acetic acid (HAc, **a**) and acetate ( $\text{Ac}^-$ , **b**) perturbation and subsequent respiration on seawater DIC and  $p\text{CO}_2$  changes. The solid lines are DIC (black) and  $p\text{CO}_2$  (grey horizontal) after the perturbation of acetic acid and equilibration with 400  $\mu\text{atm}$  atmosphere. The dashed lines are DIC (black) and  $p\text{CO}_2$  (grey) after the added HAc (or  $\text{Ac}^-$ ) is converted to  $\text{CO}_2$  (or carbonate alkalinity) in a closed system. Simulation condition,  $\text{TA} = 2350 \mu\text{mol kg}^{-1}$ ,  $S = 35$ ,  $T = 15^\circ\text{C}$ , acetic acid  $pK_a = 4.76$



degradation of large organic acid molecules that have carboxyl groups, including their conjugate bases, would lead to an initial seawater  $p\text{CO}_2$  increase and  $\text{CO}_2$  degassing, irrespective of the degradation mechanism. The same conclusion may also be drawn for phenolic compounds (another type of proton donor among natural organic acids) because their degradation may involve production of aliphatic acids as the intermediates (van Schie and Young 2000), and subsequent reaction would then have the same effect on seawater  $\text{CO}_2$  system, as DIC production from decarboxylation reactions may occur.

#### 4.6 Caveats

In natural waters, organic acids often appear in clusters with a wide range of  $pK_a$  values, some of which can be lower than 4.5 (Table 1). This study only deals with minimum  $pK_a$  at 4.5, at which pH a hypothetical acid would have equal concentrations of HOA and  $\text{OA}^-$  at the empirically defined “zero proton level” (Dickson 1981), which is widely used in determining alkalinity of natural waters. However, in cases that involve organic acids that have lower  $pK_a$  things become more challenging especially from the analytical point of view. Current curve fitting of the potentiometric titration data for alkalinity analysis uses the final pH of  $\sim 3.0$ , at which the concentrations of the major conjugate anions ( $\text{HCO}_3^-$ ) common in seawater or freshwater with little organic matter is minimal (Dickson et al. 2007). If significant quantities of organic acids are present in seawater, the species with lower  $pK_a$  ( $\leq 4.5$ ) will continue to protonate after the empirical zero proton level is reached through acid titration (Ulfsbo et al. 2015). For example, at the lower pH limit of current curve fitting scheme (pH 3.0), the unprotonated conjugate base would be about 1/32 of its protonated counterpart (if  $pK_a=4.5$ ), and the ratio would be 1/10 at pH 3.5. Hence, the currently accepted zero proton level theoretically prevents the inclusion of the bases of stronger conjugate acids. However, if these “protonation capacities” that are not included in current alkalinity titration results are present in the anionic form, upon transformation in the ocean water, it will turn out to be “excess” alkalinity through charge transfer (Hu and Cai 2011), a process in which even the conjugate base ( $\text{SO}_4^{2-}$ ) of the strong sulfuric acid can be converted to bicarbonate upon complete reduction and removal from the water column. Therefore, the problem now is how much this unrecognized protonation capacity due to the presence of conjugate bases of stronger acids (with  $pK_a < 4.5$ ) is present in river waters, which then contributes to the oceanic alkalinity cycle. This could be a potentially interesting topic for future studies.

The simple simulations using the model compounds in Sect. 4.5 do not necessarily reflect what occurs under natural conditions, and it is also widely recognized that organic alkalinity may be present even in oligotrophic ocean waters, even though their levels can be very low (Fong and Dickson 2019). However, from the buffer examination and the potential transformation to organic alkalinity in the ocean, it is unlikely that the contribution of organic alkalinity would exert major control on seawater  $\text{CO}_2$  uptake capacity.

### 5 Conclusions

Using numerical simulation, two types of organic alkalinity input (direct organic acid input, HOA, or that of its conjugate base,  $\text{OA}^-$ ) are explored for the effects on seawater carbonate chemistry under both closed-system and open-system conditions. Addition of HOA would increase seawater  $p\text{CO}_2$  in a closed system, and degassing would occur if the system

is then open to the atmosphere. In the open system scenario, if the  $pK_a$  of HOA is above a threshold value (7.15 for the simulated seawater in this work), the organic acid-perturbed seawater will have higher buffer capacity than the unperturbed one despite its lower pH. On the other hand, addition of conjugate base  $OA^-$  increases pH and decreases  $pCO_2$ . The resulting seawater will have higher buffer capacity than the unperturbed one across all simulating  $pK_a$ .

Simulations on both HOA and  $OA^-$  perturbations suggest that highest buffer occurs at organic acid  $pK_a$  8.2–8.3 when the seawater is exposed to atmospheric  $pCO_2$  of 400  $\mu\text{atm}$ .  $pK_a$  for maximum buffer is slightly dependent on the physical conditions (temperature and salinity). However, stronger organic acid (lower  $pK_a$ ) and conjugate base would play a more important role in regulating seawater buffer when  $pCO_2$  increases, or ocean acidification progresses further.

In the estuarine zone, terrestrially derived organic acids, regardless of their dissociation constants, all lead to a more acidified condition ( $CO_2$  degassing and lower pH) than the scenario in which mixing occurs between zero- $T_{HOA}$  river water and seawater. This effect diminishes with increasing salinity. Nevertheless, organic alkalinity with  $pK_a$  that provides maximum buffer in seawater would provide greater buffer in the estuarine mixing zone, while that from a stronger acid either substantially increases  $pCO_2$  at low salinity or decreases buffer against further pH change at mid to high salinity conditions.

Despite that HOA or  $OA^-$  addition could enhance seawater buffer capacity to various extents, degradation of organic acid should have a net increase in DIC. Therefore, organic alkalinity likely should not be considered as a mechanism for enhancing long-term seawater buffer or facilitating additional atmospheric  $CO_2$  uptake. Regardless, there are still many unknowns with organic alkalinity; thus, it is worth continuing investigation on how much of this alkalinity, both those organics that have been included by the current analytical approaches and those that are not (i.e.,  $pK_a$  below the currently defined zero proton level), contribute to the oceanic alkalinity cycle.

**Acknowledgements** This study is funded by the National Science Foundation Chemical Oceanography Program (OCE-1654232). The author wishes to thank Drs. David Burdige and Robert Byrne for their helpful comments on an earlier draft of this manuscript, and Melissa McCutcheon for her editorial help. Three reviewers and the associate editor provided critical insights on an earlier version of this manuscript, which helped to improve the quality of the work.

## References

- Abril G et al (2015) Technical note: large overestimation of  $pCO_2$  calculated from pH and alkalinity in acidic, organic-rich freshwaters. *Biogeosciences* 12:67–78
- Amon RMW, Benner R (1996) Photochemical and microbial consumption of dissolved organic carbon and dissolved oxygen in the Amazon River system. *Geochim Cosmochim Acta* 60:1783–1792
- Ben-Yaakov S (1973) pH buffering of pore water of recent anoxic marine sediments. *Limnol Oceanogr* 18:86–94
- Borges AV, Schiettecatte LS, Abril G, Delille B, Gazeau F (2006) Carbon dioxide in European coastal waters. *Estuar Coast Shelf Sci* 70:375–387
- Boudreau BP, Canfield DE (1993) A comparison of closed- and open-system models for porewater pH and calcite-saturation state. *Geochim Cosmochim Acta* 57:317–334
- Butman D, Raymond PA (2011) Significant efflux of carbon dioxide from streams and rivers in the United States. *Nat Geosci* 4:839–842
- Cai W-J, Yongchen W, Hodson RE (1998) Acid-base properties of dissolved organic matter in the estuarine waters of Georgia, USA. *Geochim Cosmochim Acta* 62:473–483

- Dickson AG (1981) An exact definition of total alkalinity, and a procedure for the estimation of alkalinity and total inorganic carbon from titration data. *Deep Sea Res* 28:609–623
- Dickson AG (1992) The development of the alkalinity concept in marine chemistry. *Mar Chem* 40:49–63
- Dickson AG, Millero FJ (1987) A comparison of the equilibrium constants for the dissociation of carbonic acid in seawater media. *Deep Sea Res* 34:1733–1743
- Dickson AG, Wesolowski DJ, Palmer DA, Mesmer RE (1990) Dissociation constant of bisulfate ion in aqueous sodium chloride solutions to 250.degree.C. *J Phys Chem* 94:7978–7985
- Dickson AG, Sabine CL, Christian JR (eds) (2007) Guide to best practices for ocean CO<sub>2</sub> measurements. PICES Special Publication 3, 191 pp. [https://www.noaa.gov/ocads/oceans/Handbook\\_2007.html](https://www.noaa.gov/ocads/oceans/Handbook_2007.html)
- Egleston ES, Sabine CL, Morel FMM (2010) Revelle revisited: buffer factors that quantify the response of ocean chemistry to changes in DIC and alkalinity. *Glob Biogeochem Cycle*. <https://doi.org/10.1029/2008GB003407>
- Fichot CG, Benner R (2014) The fate of terrigenous dissolved organic carbon in a river-influenced ocean margin. *Glob Biogeochem Cycle* 28:300–318
- Fong MB, Dickson AG (2019) Insights from GO-SHIP hydrography data into the thermodynamic consistency of CO<sub>2</sub> system measurements in seawater. *Mar Chem* 211:52–63
- Frankignoulle M (1994) A complete set of buffer factors for acid/base CO<sub>2</sub> system in seawater. *J Mar Syst* 5:111–118
- Hagens M, Middelburg JJ (2016) Generalised expressions for the response of pH to changes in ocean chemistry. *Geochim Cosmochim Acta* 187:334–349
- Hagens M, Hunter KA, Liss PS, Middelburg JJ (2014) Biogeochemical context impacts seawater pH changes resulting from atmospheric sulfur and nitrogen deposition. *Geophys Res Lett* 41:935–941
- Hammer K, Schneider B, Kuliński K, Schulz-Bull DE (2017) Acid-base properties of Baltic Sea dissolved organic matter. *J Mar Syst* 173:114–121
- Hernández-Ayon JM, Zirino A, Dickson AG, Camiro-Vargas T, Valenzuela-Espinoza E (2007) Estimating the contribution of organic bases from microalgae to the titration alkalinity in coastal seawaters. *Limnol Oceanogr Methods* 5:225–232
- Hofmann AF, Middelburg JJ, Soetaert K, Wolf-Gladrow DA, Meysman FJR (2010) Proton cycling, buffering, and reaction stoichiometry in natural waters. *Mar Chem* 121:246–255
- Hofmann GE et al (2011) High-frequency dynamics of ocean pH: a multi-ecosystem comparison. *PLoS ONE* 6:e28983
- Hu X, Cai W-J (2011) An assessment of ocean margin anaerobic processes on oceanic alkalinity budget. *Glob Biogeochem Cycle*. <https://doi.org/10.1029/2010GB003859>
- Hu X, Cai W-J (2013) Estuarine acidification and minimum buffer zone—a conceptual study. *Geophys Res Lett* 40:5176–5181
- Hunt CW, Salisbury JE, Vandemark D (2011) Contribution of non-carbonate anions to river alkalinity and overestimation of pCO<sub>2</sub>. *Biogeosciences* 8:3069–3076
- Jiang L-Q, Cai W-J, Wang Y (2008) A comparative study of carbon dioxide degassing in river- and marine-dominated estuaries. *Limnol Oceanogr* 53:2603–2615
- Jourabchi P, Van Cappellen P, Regnier P (2005) Quantitative interpretation of pH distributions in aquatic sediments: a reaction-transport modeling approach. *Am J Sci* 305:919–956
- Kim H-C, Lee K (2009) Significant contribution of dissolved organic matter to seawater alkalinity. *Geophys Res Lett* 36:L20603. <https://doi.org/10.21029/22009GL040271>
- Kim H-C, Lee K, Choi W (2006) Contribution of phytoplankton and bacterial cells to the measured alkalinity of seawater. *Limnol Oceanogr* 51:331–338
- Ko YH, Lee K, Eom KH, Han I-S (2016) Organic alkalinity produced by phytoplankton and its effect on the computation of ocean carbon parameters. *Limnol Oceanogr* 61:1462–1471
- Kuliński K, Schneider B, Hammer K, Machulik U, Schulz-Bull D (2014) The influence of dissolved organic matter on the acid–base system of the Baltic Sea. *J Mar Syst* 132:106–115
- Lukawska-Matuszewska K (2016) Contribution of non-carbonate inorganic and organic alkalinity to total measured alkalinity in pore waters in marine sediments (Gulf of Gdansk, S-E Baltic Sea). *Mar Chem* 186:211–220
- Lundegard PD, Land LS (1989) Carbonate equilibria and pH buffering by organic acids—response to changes in pCO<sub>2</sub>. *Chem Geol* 74:277–287
- Mehrback C, Culberson CH, Hawley JE, Pytkowicz RM (1973) Measurement of the apparent dissociation constants of carbonic acid in seawater at atmospheric pressure. *Limnol Oceanogr* 18:897–907
- Millero FJ (1979) The thermodynamics of the carbonate system in seawater. *Geochim Cosmochim Acta* 43:1651–1661
- Millero FJ (1983) The estimation of the pK\*HA of acids in seawater using the Pitzer equations. *Geochim Cosmochim Acta* 47:2121–2129

- Millero FJ (2001) Physical chemistry of natural waters. Wiley-Interscience series in geochemistry. Wiley-Interscience, New York
- Muller FLL, Bleie B (2008) Estimating the organic acid contribution to coastal seawater alkalinity by potentiometric titrations in a closed cell. *Anal Chim Acta* 619:183–191
- Nydhall AC, Wallin MB, Weyhenmeyer GA (2017) No long-term trends in  $p\text{CO}_2$  despite increasing organic carbon concentrations in boreal lakes, streams, and rivers. *Glob Biogeochem Cycle* 31:985–995
- Perdue EM, Reuter JH, Ghosal M (1980) The operational nature of acidic functional group analyses and its impact on mathematical descriptions of acid–base equilibria in humic substances. *Geochim Cosmochim Acta* 44:1841–1851
- Revelle R, Suess H (1957) Carbon dioxide exchange between atmosphere and ocean and the question of an increase of atmospheric  $\text{CO}_2$  during the past decades. *Tellus* 9:18–27
- Ritchie JD, Perdue EM (2003) Proton-binding study of standard and reference fulvic acids, humic acids, and natural organic matter. *Geochim Cosmochim Acta* 67:85–96
- Serjeant EP, Dempsey B (1979) Ionisation constants of organic acids in aqueous solution, vol 23. Pergamon, New York
- Sippo JZ, Maher DT, Tait DR, Holloway C, Santos IR (2016) Are mangroves drivers or buffers of coastal acidification? Insights from alkalinity and dissolved inorganic carbon export estimates across a latitudinal transect. *Glob Biogeochem Cycle* 30:753–766
- Stumm W, Morgan JJ (1995) Aquatic chemistry: chemical equilibria and rates in natural waters, 3rd edn. Wiley, New York
- Ulfsson A, Kulinski K, Anderson LG, Turner DR (2015) Modelling organic alkalinity in the Baltic Sea using a Humic–Pitzer approach. *Mar Chem* 168:18–26
- Uppström LR (1974) The boron/chlorinity ratio of deep-sea water from the Pacific Ocean. *Deep-Sea Res: Oceanogr Abstr* 21:161–162
- van Heuven S, Pierrot SD, Rae JWB, Lewis E, Wallace DWR (2011) MATLAB program developed for  $\text{CO}_2$  system calculations. ORNL/CDIAC-105b., Carbon Dioxide Information Analysis Center, Oak Ridge National Laboratory, US DoE, Oak Ridge, TN. <https://doi.org/10.1002/2014GB004868>
- van Schie PM, Young LY (2000) Biodegradation of phenol: mechanisms and applications. *Bioremediat J* 4:1–18
- Wang ZA, Bienvenu DJ, Mann PJ, Hoering KA, Poulsen JR, Spencer RGM, Holmes RM (2013) Inorganic carbon speciation and fluxes in the Congo River. *Geophys Res Lett* 40:511–516
- Wang ZA, Kroeger KD, Ganju NK, Gonanea ME, Chu SN (2016) Intertidal salt marshes as an important source of inorganic carbon to the coastal ocean. *Limnol Oceanogr* 61:1916–1931
- Welch SA, Ullman WJ (1993) The effect of organic acids on plagioclase dissolution rates and stoichiometry. *Geochim Cosmochim Acta* 57:2725–2736
- Yang B, Byrne RH, Lindemuth M (2015) Contributions of organic alkalinity to total alkalinity in coastal waters: a spectrophotometric approach. *Mar Chem* 176:199–207
- Yao H, Hu X (2017) Responses of carbonate system and  $\text{CO}_2$  flux to extended drought and intense flooding in a semiarid subtropical estuary. *Limnol Oceanogr* 62:S112–S130

**Publisher's Note** Springer Nature remains neutral with regard to jurisdictional claims in published maps and institutional affiliations.